RSC Mechanochemistry

ROYAL SOCIETY OF CHEMISTRY

COMMUNICATION

View Article Online
View Journal | View Issue

Cite this: *RSC Mechanochem.*, 2024, **1**, 322

Received 9th May 2024
Accepted 17th June 2024

DOI: 10.1039/d4mr00048j

rsc.li/RSCMechanochem

Facile mechanochemical synthesis of hypervalent tin(IV)-fused azo/azomethine compounds showing solid-state emission†

Masayuki Gon, Taichi Kato, Kazuya Tanimura, Chiaki Hotta and Kazuo Tanaka *

Mechanochemical synthesis involves carrying out chemical reactions without solvents and has attracted much attention as green chemistry. Herein, we demonstrate solvent- and catalyst-free mechanochemical synthesis of hypervalent tin(IV) compounds with azo/azomethine tridentate ligands and organotin(IV) oxide by manual grinding in an agate mortar. FT-IR spectra indicate that 41–82% of the ligands can be converted to hypervalent tin compounds depending on the reaction conditions. The resulting products exhibit solid-state emission in the yellow to deep-red region without purification.

1. Introduction

Solid-state mechanochemical reactions have attracted much attention as environmentally friendly reactions where organic solvents can be dramatically saved compared to solution processes.[1,2] The solid-state reactions proceed *via* contact between solid reactants, and a large number of organic reactions have been accomplished.[3–7] Although solution processes have been a general approach for soluble reactants, unique mechanochemical reactions have been discovered in recent years, and the same products are hardly accessible in solution processes.[8–12] Catalyst-free mechanochemistry has been proposed as a powerful green chemical tool with high atom economy,[13] and various types of luminescent organic dyes[14–18] and metal complexes[19–23] have been synthesized. Mechanochemistry still has benefits in the development of new materials taking advantage of its usefulness and originality, and the discovery of solid-state reactions to directly produce functional materials that can be used without purification is still highly desired in terms of cost and energy reductions.[1,24]

We have recently reported the synthesis of five-coordinated hypervalent tin(IV) compounds by using O,N,O-tridentate ligands based on azobenzene π-conjugated systems.[25–27] It is known that the reaction has high atom economy and proceeds effectively by catalyst-free dehydration condensation in the solution processes.[28–30] The hypervalent tin compounds show unique optical properties resulting from the three-center four-electron (3c–4e) and the tin–nitrogen (Sn–N) bonds around the hypervalent tin center, such as deep-red emission and stimuli-responsiveness with the reversible coordination-number shift from five to six.[25–27] Moreover, we have also prepared hypervalent germanium(IV)[31,32] and bismuth(III)[33] compounds which exhibited near-infrared (NIR) emission and higher Lewis acidity, respectively, compared to the tin analogs. Mechanochemical reactions in the main-group elements have been actively studied,[2] and organotin compounds can also be prepared by combining various types of ligands.[34–36] Since the O,N,O-tridentate ligands show high reactivity toward the heteroatom-based reactants, even toward the poorly soluble organotin(IV) oxide in common organic solvents,[37,38] it is expected that an atom–economical reaction can be realized in the solid state.

Herein, we demonstrate the solid-state mechanochemical reaction between azo/azomethine π-conjugated tridentate ligands and diphenyltin(IV) oxide. It was found that the reaction proceeds effectively by manual grinding with weak forces in an agate mortar. The product yields were estimated by using FT-IR spectra and improved by increasing the amount of diphenyltin(IV) oxide and using liquid-assisted grinding (LAG) conditions.[39] This reaction is environmentally friendly because the by-product of this reaction is only water, and the mechanically mixed products can be used directly as luminescent materials without energy-consuming purification processes. Our results should be one of the examples of a green chemical approach to produce functional materials with high atom economy and low environmental burden.

2. Materials and methods

2.1 General methods

Solid-state ^{119}Sn cross-polarization (CP) magic angle spinning (MAS) NMR spectra were recorded on a Bruker AVANCE600

Department of Polymer Chemistry, Graduate School of Engineering, Kyoto University Katsura, Nishikyo-ku, Kyoto 615-8510, Japan. E-mail: tanaka@poly.synchem.kyoto-u.ac.jp

† Electronic supplementary information (ESI) available. See DOI: https://doi.org/10.1039/d4mr00048j

instrument at 224 MHz using Me_4Sn (0 ppm) as an external standard. High-resolution mass spectrometry (HRMS) was performed at the Technical Support Office (Department of Synthetic Chemistry and Biological Chemistry, Graduate School of Engineering, Kyoto University), and the HRMS spectra were obtained on a Thermo Fisher Scientific EXACTIVE spectrometer for Direct Analysis in Real Time (DART). UV-vis absorption and diffuse reflectance UV-vis absorption spectra were recorded on a SHIMADZU UV-3600i Plus spectrophotometer, and the samples were analyzed at room temperature. Fluorescence emission spectra were recorded on a HORIBA Scientific Fluorolog-3 spectrofluorometer and the samples were analyzed at room temperature with PMT P928 as a detector. Absolute photoluminescence quantum efficiency (Φ_{PL}) was recorded on a Hamamatsu Photonics Quantaurus-QY Plus C13534-01. Powder Xray diffraction (PXRD) patterns were taken by using CuKα radiation with a Rigaku Miniflex. Fourier transform infrared (FT-IR) spectra were recorded on a Shimadzu IRPrestige-21 by preparing KBr pellets.

2.2 Materials

As the reactants, 2,2′-dihydroxyazobenzene (**^{L}Az**) (Sigma-Aldrich), *o*-salicylideneaminophenol (**^{L}Am**) (FUJIFILM Wako Pure Chemical Corporation), and diphenyltin(IV)oxide (**1**) (Sigma-Aldrich) were purchased and used without purification. Acetone (deoxidized grade, FUJIFILM Wako Pure Chemical Corporation) was purchased and used as the solvent without purification. **SnAz-SP**[25] and **SnAm-SP**[40] were prepared as described in the literature.

2.3 Experimental procedure

2.3.1 General procedure of mechanochemical synthesis. A mixture of *o*-salicylideneaminophenol (**^{L}Am**) (100 mg, 0.469 mmol, 1.0 eq.) and diphenyltin(IV) oxide (**1**) (condition A: 135 mg, 0.469 mmol, 1.0 eq. condition B: 244 mg, 0.844 mmol, 1.8 eq. condition C: 244 mg, 0.844 mmol, 1.8 eq. with 2 drops of acetone (30 μL)) was placed in an agate mortar. The mixture was reacted by manual grinding for at least 30 minutes until the reactants became a homogeneous powder. The resulting powder was allowed to stand for at least 1 day to finish the reaction. The obtained powder was analyzed without further purification.

3. Results and discussion

3.1 Synthesis

Hypervalent tin(IV)-fused azobenzene (**SnAz**) and azomethine (**SnAm**) were synthesized by manual grinding with the corresponding ligand, 2,2′-dihydroxyazobenzene (**^{L}Az**, 100 mg) and *o*-salicylideneaminophenol (**^{L}Am**, 100 mg), in the presence of diphenyltin(IV) oxide (**1**) in an agate mortar, respectively (Scheme 1). Interestingly, it was demonstrated that the reaction proceeded just by application of weak mechanical forces to the mixture of **^{L}Az** and **1** (Movie 1†). At the initial stage, an emission color change to red, which represents the generation of the hypervalent tin(IV) compound, was already recognized. Therefore, we found that this compound pair has high reactivity in mechanochemical treatments. To gather systematic information, reactions were performed under three different conditions; A: 1/1 mol mol^{-1} mixing (the equivalent condition, **SnAz-A** and **SnAm-A**); B: 1/1.8 mol mol^{-1} mixing (the excess ligand condition, **SnAz-B** and **SnAm-B**); C: 1/1.8 mol mol^{-1} mixing with 2 drops of acetone (30 μL) (the LAG condition, **SnAz-C** and **SnAm-C**). Pure **SnAz** and **SnAm** (**SnAz-SP** and **SnAm-SP**) were also prepared by conventional solution processes according to the literature.[25,40] In the previous report, a long and sufficient reaction time (3 h) for the solution process was employed to complete the reaction.[25] In the mechanochemical reaction, the reaction would immediately resume after the ground reagents are dispersed in the solution to isolate the products. Therefore it is difficult to precisely determine reaction yields. Hence, all characterization data of the mechanochemical products were measured in the solid without additional purification. The mechanochemical products were stable because the hypervalent tin compounds have ring-fused structures and are inactive to the reactants (ligands and diphenyltin(IV) oxide). In addition, all compounds are stable in air.

3.2 Characterization by MS, PXRD, and FT-IR measurements

First, we confirmed the progress of the mechanochemical reactions to produce hypervalent tin compounds by solid-state direct analysis with real time (DART) mass spectroscopy (MS) (Fig. S1†). Even in the equivalent condition A, the signals originating from the products were detected at 486.0399 for **SnAz** $[M]^-$ and at 486.0516 for **SnAm** $[M + H]^+$. Moreover, the obtained signal patterns were identical to the simulated patterns. These results prove that the dehydration condensation between each ligand and **1** should proceed by simple manual grinding. To obtain further information about the products through condition A, solid-state ^{119}Sn CP/MAS NMR spectrum measurements were conducted (Fig. S2†).[41–43] The signals derived from the mixture of **1** and **SnAz** and **SnAm** were detected from the products. This means that **SnAz** and **SnAm** should be produced through condition A, while the unreacted ligands and **1** remained. The reaction progress was also confirmed by the powder X-ray diffraction (PXRD) analysis. As a result, the products had the signals assigned to **SnAz** and **SnAm** in addition to those assigned to the reactants **1** and **^{L}Az** and **^{L}Am**, respectively (Fig. S3†). Although it can be presumed that the ground samples might lose their crystallinity and form amorphous states, the generation of the new peaks derived from

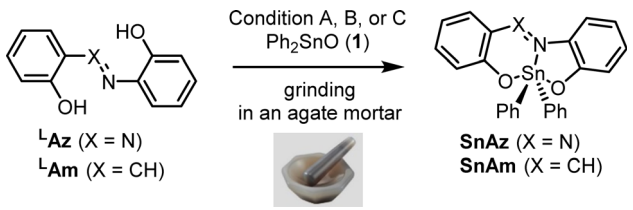

Scheme 1 Mechanochemical synthesis of **SnAz** and **SnAm**. Condition A: L/**1** = 1/1 mol mol^{-1}, condition B: L/**1** = 1/1.8 mol mol^{-1}, condition C: L/**1** = 1/1.8 mol mol^{-1} with 2 drops of acetone (30 μL). L: **^{L}Az** or **^{L}Am**.

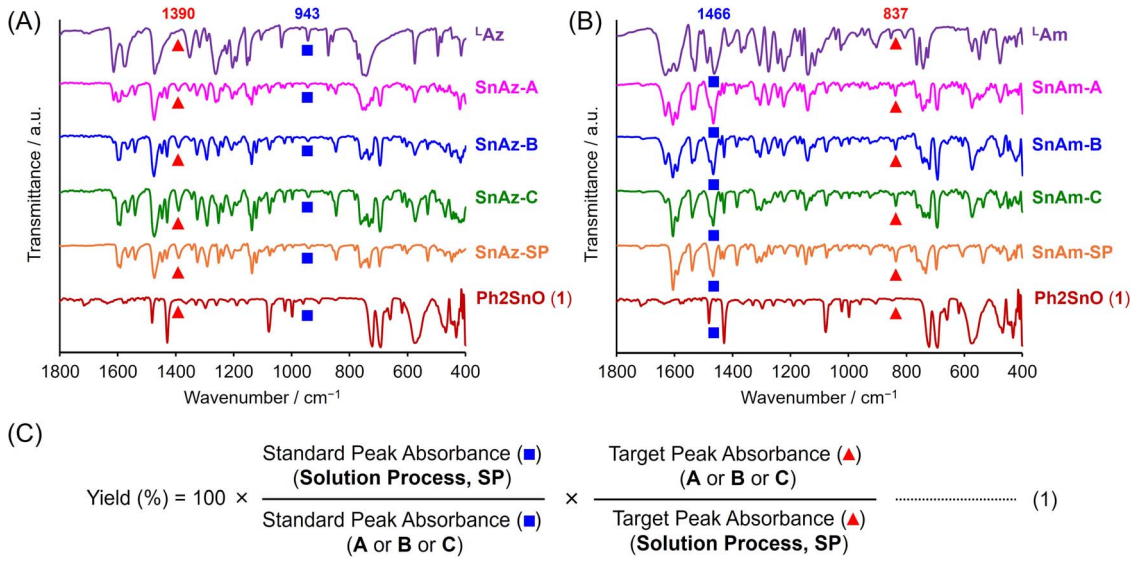

Fig. 1 FT-IR spectra of (A) ^{L}Az, SnAz-A, B, C and SP, and Ph2SnO (1), (B) ^{L}Am, SnAm-A, B, C and SP, and Ph2SnO (1). (C) Chemical formula for calculating the yields of mechanochemical reactions under various conditions. Square and triangle marks denote standard peaks and target peaks, respectively. Standard peak: originating from both the precursor (^{L}Az or ^{L}Am) and the products (A, B, C, and solution process, SP). Target peak: originating only from product (A, B, C, and solution process, SP). Ph2SnO (1) has neither standard peaks nor target peaks.

SnAz and **SnAm** was observed under all conditions A, B, and C, meaning that regular structures should be formed. This fact implies that the mechanochemical contact between the reactants by manual grinding could provide sufficient mobility of the molecules to orientate regular structures followed by crystalline states.[44]

Next, the product yields of the mechanochemical reactions under each condition were estimated by FT-IR using eqn (1) (Fig. 1 and Table 1). By comparing each spectrum of the ligands (**^{L}Az** and **^{L}Am**), the pure product (**SnAz-SP** and **SnAm-SP**) and **1**, the signal peaks at 1390 cm^{-1} and 837 cm^{-1} were selected as a target originating from the product, respectively. In addition, the signal peaks at 943 cm^{-1} and 1466 cm^{-1} were chosen as a standard remaining before and after the reaction, to calculate the yields of **SnAz** and **SnAm**, respectively. Consequently, the mechanochemical reactions proceeded 41% even under the equivalent condition (condition A) for **SnAz** and **SnAm**. The yields increased on using an excess amount of **1** (condition B) and the LAG (condition C), and finally higher reaction yields in 82% and 72% were observed for **SnAz-C** and **SnAm-C**, respectively. These results suggest that the dehydration condensation reaction should proceed effectively by manual grinding in the agate mortar and subsequently form ordered structures. Moreover, it was found that the LAG plays a positive role in the reaction progresses.

3.3 Optical properties

To evaluate the optical properties of the mechanochemically synthesized products, we performed diffuse reflectance UV-vis absorption and photoluminescence (PL) spectrum measurements with the solid samples and compared their spectra to those of **SnAz-SP** and **SnAm-SP**. As a result, all products showed luminescence from the yellow to deep-red region (Fig. 2 and Table 2). In particular, the products exhibited similar absorption and PL bands regardless of the reaction conditions. In UV-vis absorption spectra, the bands in the solid samples were broader than those in solution. This is likely due to intermolecular interactions between the chromophores (Fig. 2A and D). In contrast, in PL spectra, the bands in the solid samples were sharper than those in solution. This is probably because of the effect of self-absorption and suppression of structural relaxation in the excited state (Fig. 2B and E). The broadest absorption

Table 1 Calculated yields of mechanochemical reactions from FT-IR data

	Abs. at 943 cm^{-1} (standard)[a]	Abs. at 1390 cm^{-1} (target)[a]	Yield[b]/%		Abs. at 1466 cm^{-1} (standard)[a]	Abs. at 837 cm^{-1} (target)[a]	Yield[b]/%
SnAz-A	0.038	0.071	41	**SnAm-A**	0.73	0.12	41
SnAz-B	0.040	0.10	57	**SnAm-B**	0.61	0.13	51
SnAz-C	0.061	0.23	82	**SnAm-C**	0.52	0.15	72
SnAz-SP	0.030	0.14	—	**SnAm-SP**	0.43	0.17	—

[a] Absorbance (Abs.) = 2 − log(transmittance/%). [b] Based on the ligands.

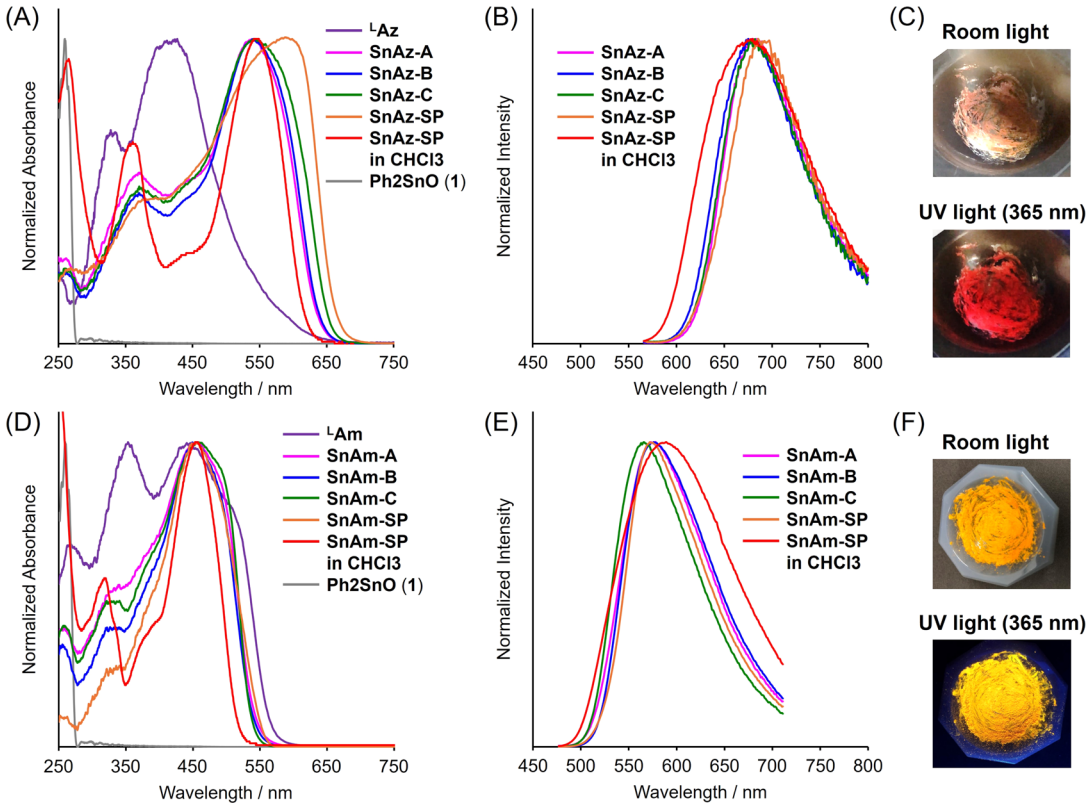

Fig. 2 (A) Normalized diffuse reflectance UV-vis absorption spectra of ^{L}Az, SnAz-A, B, C and SP, and 1 in the solid state, and normalized UV-vis absorption spectra of SnAz-SP in $CHCl_3$ solution (1.0×10^{-5} M). (B) Normalized PL spectra of SnAz-A, B, C and SP in the solid state and SnAz-SP in $CHCl_3$ solution (1.0×10^{-5} M), excited at λ_{abs}. (C) Photographs of the sample (SnAz) reacted by manual grinding in an agate mortar. (D) Normalized diffuse reflectance UV-vis absorption spectra of ^{L}Am, SnAm-A, B, C and SP, and 1 in the solid state, and normalized UV-vis absorption spectra of SnAm-SP in $CHCl_3$ solution (1.0×10^{-5} M). (E) Normalized PL spectra of SnAm-A, B, C and SP in the solid state and SnAm-SP in $CHCl_3$ solution (1.0×10^{-5} M), excited at λ_{abs}. (F) Photographs of the sample (SnAm) reacted by manual grinding in an agate mortar.

bands in **SnAz-SP** and **SnAm-SP** were attributed to strong intermolecular interactions because of their high crystallinity.

In **SnAz**, the values of the absolute PL quantum yield (Φ_{PL}) of all products were similar (Table 2). However, in **SnAm**, lower Φ_{PL} values were observed from the mechanochemically synthesized products. This is probably due to the self-absorption of luminescence caused by the non-emissive unreacted ligand (^{L}**Am**). Indeed, the Φ_{PL} of the 1/1 mol mol^{-1} grinding sample of ^{L}**Am** and **SnAm-SP** was reduced to 7.0% (the Φ_{PL} of **SnAm-SP**: 26.4%). Since the absorption band of ^{L}**Az** hardly overlaps with those of the products (**SnAz**), self-absorption hardly occurs in the solid samples. On the other hand, the overlapped absorption band of ^{L}**Am** with those of the products (**SnAm**) should induce critical reductions of the Φ_{PL} values. It should be mentioned that slightly high Φ_{PL} values were observed for **SnAz-B** and **SnAz-C**. These enhancements could be derived from the suppression of the aggregation-caused quenching by dispersing the luminophores, **SnAz-B** and **SnAz-C**, in **1** which hardly absorbs the excitation light.[45] From the time course profile of the mechanochemical reaction to prepare **SnAm-A**, the Φ_{PL} rose gradually with increasing reaction time, and at least 30 min and 1 day standing time were required to obtain the nearly saturated

Table 2 Optical data of the products prepared under various conditions and using various reactants

	$\lambda_{abs}{}^{a}$/nm	$\lambda_{PL}{}^{c}$/nm	$\Phi_{PL}{}^{c,d}$/%		$\lambda_{abs}{}^{a}$/nm	$\lambda_{PL}{}^{c}$/nm	$\Phi_{PL}{}^{c,d}$/%
^{L}**Az**	427	n.d^{e}	n.d^{e}	^{L}**Am**	446	n.d^{e}	n.d^{e}
SnAz-A	541	683	3.2	**SnAm-A**	455	578	8.8
SnAz-B	541	675	4.0	**SnAm-B**	454	576	11.8
SnAz-C	543	682	4.2	**SnAm-C**	455	566	18.6
SnAz-SP	589	685	3.7	**SnAm-SP**	457	572	26.4
SnAz-SP^{b}	545^{b}	680^{b}	3.5^{b}	**SnAm-SP**^{c}	455^{b}	589^{b}	20.5^{b}
Ph2SnO (1)	260	n.d^{e}	n.d^{e}				

^{a} Solid dispersed in $BaSO_4$. ^{b} 1.0×10^{-5} M in $CHCl_3$. ^{c} Excited at λ_{abs}. ^{d} Absolute PL quantum yield excited at absorption maxima. ^{e} Not detected.

properties of the mechanochemical products (Fig. S4†). In summary, the above data from optical measurements clearly indicate that solid-state luminescent materials were able to be obtained directly from the mechanochemical reactions.

4. Conclusions

In this manuscript, we demonstrated that hypervalent tin compounds are able to be formed by manual grinding with weak forces in the solid state, and the products are directly used as a luminescent material without further purification. Since this reaction proceeds by dehydration condensation without organic solvents and the products were obtained without energy-consuming purification processes, it can be said that our synthetic methods are a green chemical approach for material production with low environmental impact and high atomic efficiency. Moreover, mechanochemical reactions are often applicable for synthesizing unstable complexes which are rapidly degraded in solution. Our findings might be versatile for constructing novel π-conjugated systems containing hypervalent tin complexes.

Data availability

All experimental and characterization data and detailed experimental procedures are available in the published article and ESI.†

Author contributions

M. G. wrote the original draft, conducted the data analysis, and performed additional experiments. T. K. synthesized the compounds, performed the experiments and conducted the data analysis. K. T. (Kazuya Tanimura) and C. H. performed additional experiments. K. T. (Kazuo Tanaka) supervised the project. All the authors discussed the results and contributed to editing the manuscript.

Conflicts of interest

There are no conflicts to declare.

Acknowledgements

This work was partially supported by the Izumi Science and Technology Foundation (for M. G.), Japan Society for the Promotion of Science (JSPS), a Grant-in-Aid for Scientific Research (B) (for M. G.) (JP23K23398) and (for K. T.) (JP24K01570).

Notes and references

1 S. L. James, C. J. Adams, C. Bolm, D. Braga, P. Collier, T. Friščić, F. Grepioni, K. D. M. Harris, G. Hyett, W. Jones, A. Krebs, J. Mack, L. Maini, A. G. Orpen, I. P. Parkin, W. C. Shearouse, J. W. Steed and D. C. Waddell, *Chem. Soc. Rev.*, 2012, **41**, 413–447.
2 D. Tan and F. García, *Chem. Soc. Rev.*, 2019, **48**, 2274–2292.
3 G.-W. Wang, *Chem. Soc. Rev.*, 2013, **42**, 7668–7700.
4 J. L. Howard, Q. Cao and D. L. Browne, *Chem. Sci.*, 2018, **9**, 3080–3094.
5 N. Dey, A. Mandal, R. Jana, A. Bera, S. A. Azad, S. Giri, M. Ikbal and S. Samanta, *New J. Chem.*, 2023, **47**, 13035–13079.
6 D. Margetić, *Pure Appl. Chem.*, 2023, **95**, 315–328.
7 F. Cuccu, L. De Luca, F. Delogu, E. Colacino, N. Solin, R. Mocci and A. Porcheddu, *ChemSusChem*, 2022, **15**, e202200362.
8 S. Ishikawa, D. Sakamaki, M. Gon, K. Tanaka and H. Fujiwara, *Chem. Commun.*, 2024, **60**, 4946–4949.
9 Y. Gao, K. Kubota and H. Ito, *Angew. Chem., Int. Ed.*, 2023, **62**, e202217723.
10 T. Seo, N. Toyoshima, K. Kubota and H. Ito, *J. Am. Chem. Soc.*, 2021, **143**, 6165–6175.
11 P. Gao, J. Jiang, S. Maeda, K. Kubota and H. Ito, *Angew. Chem., Int. Ed.*, 2022, **61**, e202207118.
12 S. Saha, A. A. Bhosle, A. Chatterjee and M. Banerjee, *J. Org. Chem.*, 2023, **88**, 10002–10013.
13 B. R. Naidu, T. Sruthi, R. Mitty and K. Venkateswarlu, *Green Chem.*, 2023, **25**, 6120–6148.
14 M. Banerjee, A. A. Bhosle, A. Chatterjee and S. Saha, *J. Org. Chem.*, 2021, **86**, 13911–13923.
15 A. A. Bhosle, S. D. Hiremath, A. C. Bhasikuttan, M. Banerjee and A. Chatterjee, *J. Photochem. Photobiol., A*, 2021, **413**, 113265.
16 A. Mahata, P. Bhaumick, A. K. Panday, R. Yadav, T. Parvin and L. H. Choudhury, *New J. Chem.*, 2020, **44**, 4798–4811.
17 Q. Cao, D. E. Crawford, C. Shi and S. L. James, *Angew. Chem., Int. Ed.*, 2020, **59**, 4478–4483.
18 A. A. Bhosle, M. Banerjee, S. D. Hiremath, A. C. Bhasikuttan and A. Chatterjee, *Chem.–Asian J.*, 2023, **18**, e202300048.
19 C. Zeng, N. Wang, T. Peng and S. Wang, *Inorg. Chem.*, 2017, **56**, 1616–1625.
20 A. Kobayashi, T. Hasegawa, M. Yoshida and M. Kato, *Inorg. Chem.*, 2016, **55**, 1978–1985.
21 P. Liang, A. Kobayashi, T. Hasegawa, M. Yoshida and M. Kato, *Eur. J. Inorg. Chem.*, 2017, **2017**, 5134–5142.
22 D. Yang, Z. Li, L. He, Y. Deng and Y. Wang, *RSC Adv.*, 2017, **7**, 14314–14320.
23 A. Deák, C. Jobbágy, A. Demeter, L. Čelko, J. Cihlář, P. T. Szabó, P. Ábrányi-Balogh, D. E. Crawford, D. Virieux and E. Colacino, *Dalton Trans.*, 2021, **50**, 13337–13344.
24 G. Kaupp, R. Naimi-Jamal and J. Schmeyers, *Tetrahedron*, 2003, **59**, 3753–3760.
25 M. Gon, K. Tanaka and Y. Chujo, *Chem.–Eur. J.*, 2021, **27**, 7561–7571.
26 M. Gon, K. Tanimura, M. Yaegashi, K. Tanaka and Y. Chujo, *Polym. J.*, 2021, **53**, 1241–1249.
27 M. Gon, Y. Morisaki, K. Tanimura, K. Tanaka and Y. Chujo, *Mater. Chem. Front.*, 2023, **7**, 1345–1353.
28 K. E. Bessler, J. A. dos Santos, V. M. Deflon, S. de Souza Lemos and E. Niquet, *Z. Anorg. Allg. Chem.*, 2004, **630**, 742–745.

29 H. Reyes, C. Garcìa, N. Farfán, R. Santillan, P. Lacroix, C. Lepetit and K. Nakatani, *J. Organomet. Chem.*, 2004, **689**, 2303–2310.
30 M. Nath and N. Chaudhary, *Synth. React. Inorg. Met.-Org. Chem.*, 1998, **28**, 121–133.
31 M. Gon, M. Yaegashi, K. Tanaka and Y. Chujo, *Chem.–Eur. J.*, 2023, **29**, e202203423.
32 M. Gon, M. Yaegashi and K. Tanaka, *Bull. Chem. Soc. Jpn.*, 2023, **96**, 778–784.
33 K. Tanimura, M. Gon and K. Tanaka, *Inorg. Chem.*, 2023, **62**, 4590–4597.
34 J. A. Cabeza, J. F. Reynes, F. García, P. García-Álvarez and R. García-Soriano, *Chem. Sci.*, 2023, **14**, 12477–12483.
35 R. F. Koby, T. P. Hanusa and N. D. Schley, *J. Am. Chem. Soc.*, 2018, **140**, 15934–15942.
36 V. Chandrasekhar, V. Baskar, R. Boomishankar, K. Gopal, S. Zacchini, J. F. Bickley and A. Steiner, *Organometallics*, 2003, **22**, 3710–3716.
37 S. Masamune, L. R. Sita and D. J. Williams, *J. Am. Chem. Soc.*, 1983, **105**, 630–631.
38 M. A. Edelman, P. B. Hitchcock and M. F. Lappert, *J. Chem. Soc., Chem. Commun.*, 1990, 1116–1118.
39 P. Ying, J. Yu and W. Su, *Adv. Synth. Catal.*, 2021, **363**, 1246–1271.
40 J. S. Zugazagoitia, M. Maya, C. Damián-Zea, P. Navarro, H. I. Beltrán and J. Peon, *J. Phys. Chem. A*, 2010, **114**, 704–714.
41 D. V. Airapetyan, V. S. Petrosyan, S. V. Gruener, A. A. Korlyukov, D. E. Arkhipov, A. A. Bowden and K. V. Zaitsev, *Inorg. Chim. Acta*, 2015, **432**, 142–148.
42 P. Kitschke, A.-M. Preda, A. A. Auer, S. Scholz, T. Rüffer, H. Lang and M. Mehring, *Dalton Trans.*, 2019, **48**, 220–230.
43 J. Henning, H. Schubert, K. Eichele, F. Winter, R. Pöttgen, H. A. Mayer and L. Wesemann, *Inorg. Chem.*, 2012, **51**, 5787–5794.
44 T. Friščić and W. Jones, *Cryst. Growth Des.*, 2009, **9**, 1621–1637.
45 S. A. Jenekhe and J. A. Osaheni, *Science*, 1994, **265**, 765–768.